The lung environment controls alveolar macrophage metabolism and responses in type 2 inflammation

Freya R. Svedberg[1$&], Sheila L. Brown[1], Maria Z. Krauss[2], Laura Campbell[2], Catherine Sharpe[2], Maryam Clausen[3], Gareth J. Howell[1], Howard Clark[4], Jens Madsen[4], Christopher M. Evans[5], Tara E. Sutherland[1], Alasdair C. Ivens[6], David J. Thornton[2], Richard K. Grencis[2], Tracy Hussell[1], Danen M. Cunoosamy[7], Peter C. Cook[1]* and Andrew S. MacDonald[1]*.

Affiliations:

[1]Lydia Becker Institute of Immunology and Inflammation, Manchester Collaborative Centre for Inflammation Research, Faculty of Biology, Medicine and Health, University of Manchester, Manchester Academic Health Science Centre, Core Technology Facility, 46 Grafton Street, Manchester M13 9NT, UK.

[2]Lydia Becker Institute of Immunology and Inflammation, Wellcome Trust Centre for Cell-Matrix Research, Faculty of Biology, Medicine and Health, University of Manchester, Manchester Academic Health Science Centre, AV Hill Building, Manchester M13 9PT, UK.

[3]AstraZeneca, Discovery Sciences IMED, Gothenburg, Sweden.

[4]Department of Child Health, Division of Clinical and Experimental Sciences, Faculty of Medicine, Sir Henry Wellcome Laboratories, Southampton General Hospital,University of Southampton, Southampton, UK. Institute for Life Sciences, University of Southampton, Southampton, United Kingdom. National Institute for Health Research, Southampton Respiratory Biomedical Research Unit, Southampton Centre for Biomedical Research, University Hospital Southampton NHS Foundation Trust, Southampton, UK.

[5]Department of Medicine, University of Colorado School of Medicine, 12700 E 19th Avenue, Mailstop 8611, Research Complex 2, Room 3121, Aurora, Colorado 80045, USA.

[6]Institute of Immunology and Infection Research, Centre for Immunity, Infection and Evolution, School of Biological Sciences, University of Edinburgh, UK.

[7]AstraZeneca RIA IMED, Gothenburg, Sweden.

Author at current address:

[$]*Laboratory of Myeloid Cell Ontogeny and Functional Specialisation, VIB Center for Inflammation Research, Ghent, Belgium*

[&]*Department of Biomedical Molecular Biology, Ghent University, Ghent, Belgium*

*Correspondence should be addressed to P.C.C. (peter.c.cook@manchester.ac.uk) or A.S.M. (andrew.macdonald@manchester.ac.uk).

Fine control of macrophage activation is needed to prevent inflammatory disease, particularly at barrier sites such as the lungs. However, the dominant mechanisms that regulate pulmonary macrophage activation during inflammation are currently poorly understood. Here we found that alveolar macrophages were substantially less able to respond to the canonical type 2 cytokine IL-4, which underpins allergic disease and parasitic worm infections, than lung tissue or peritoneal cavity macrophages. We found that alveolar macrophage hypo-responsiveness to IL-4 was dictated by the lung environment, but was independent of the host microbiota or the lung extracellular-matrix components surfactant protein D or mucin 5b. Alveolar macrophages displayed severely dysregulated metabolism compared to that of cavity macrophages. After being removed from the lung, alveolar macrophages regained responsiveness to IL-4 in a manner dependent on glycolysis. Thus, impaired glycolysis within the pulmonary niche was a central determinant for the regulation of alveolar macrophage responsiveness during type 2 inflammation.

The specialized mucosal environment of the lung is required to enable breathing in the face of continuous exposure to debris and micro-organisms, while also calling for diverse mechanisms to restrict disease caused by over-exuberant inflammatory responses[1]. Lung macrophages have been proposed to be central to mediating and regulating type 2 inflammation against allergens and parasitic worms, which together affect billions of people worldwide[2]. Against these types of challenge, macrophages can expand *in situ* to type 2 cytokines such as IL-4 that trigger 'alternative' (or M(IL-4)) activation, linked to wound repair and type 2 pathology[3, 4, 5]. Although pulmonary macrophage sub-populations inhabit dramatically different anatomical sites, such as the airways and tissue parenchyma, it is not yet clear how location influences their ability to respond to type 2 inflammation. In particular, reports of M(IL-4) marker expression on lung macrophages during type 2 inflammation[6, 7, 8, 9] have involved experimental approaches that may not clearly distinguish macrophages from other myeloid cells, raising the possibility that functional differences in key macrophage sub-populations have been inadvertently overlooked.

As the predominant macrophage sub-population in airways, alveolar macrophages (AlvMs) are vital for maintaining lung health and function, having a central role in clearance of debris, surfactant and apoptotic cells[10]. In the absence of AlvMs, fluid build-up leads to primary pulmonary alveolar proteinosis, severe lung dysfunction and respiratory failure[11]. The majority of AlvMs are thought to be derived from embryonic precursors that seed the lung tissue before birth[12], with recent evidence suggesting that the cytokines GM-CSF and TGF-β induce PPAR-γ, a crucial transcription factor for AlvM development[11, 13, 14]. During inflammation, AlvMs mediate bacterial clearance and initiate neutrophil recruitment[15], functions that can be regulated by cytokines such as IL-10 or TGF-β, and/or the engagement of cell surface receptors such as SIRPα or CD200[16]. Because clear discrimination between AlvMs and other lung macrophage sub-populations is technically challenging[17], far less is known about the function and origin of tissue residing interstitial macrophages (IntMs). Although IntMs may comprise up to three separate sub-populations[18], earlier work may have mistakenly identified them as AlvMs, monocytes or dendritic cells (DCs).

Mucosal environments like the lung play a major role in determining both development and function of macrophages[19], though many of the factors that shape such processes remain unclear, particularly in type 2 inflammation. Lung macrophage upregulation of M(IL-4) markers during parasite-mediated type 2 responses is promoted by environmental factors such as surfactant protein A (SP-A) and engagement of TAM receptors during clearance of apoptotic cells[20, 21]. Here we show that lung macrophage subsets, particularly AlvMs, were considerably less responsive to type 2 inflammation than macrophages from other tissues. We demonstrate that this muted phenotype was conferred by the lung environment, and was independent of potential negative regulators such as CD200-CD200R, surfactant protein D (SP-D), mucin 5b (Muc5b) or the host microbiota. Hypo-responsive AlvMs had an altered metabolic profile compared to IL-4-responsive peritoneal exudate cell macrophages (PECMs), and were unable to upregulate glycolysis *in situ*.

After removal from the lung, AlvMs recovered their IL-4 responsiveness in a glycolysis-dependent manner. Thus, the pulmonary environment controlled AlvM responsiveness during type 2 inflammation via modulation of their metabolic activity.

Results

AlvMs are unresponsive to IL-4 *in vivo*

To better understand how pulmonary macrophages respond during type 2 inflammation, we utilized MerTK, CD64, Siglec-F and CD11b as markers that distinguish AlvMs from IntMs[11, 17, 18]. The majority of lung tissue and bronchoalveolar lavage (BAL) macrophages were MerTK$^+$CD64$^+$CD11b$^-$Siglec-F$^+$ AlvMs (>89%), alongside a smaller population (<10%) of MerTK$^+$CD64$^+$CD11b$^+$Siglec-F$^-$ IntMs (Fig. 1a,b and Supplementary Fig. 1a). Analysis of additional macrophage markers showed that, while both AlvMs and IntMs expressed F4/80 and CD11c, AlvMs were also Ym1^{hi}, a feature of M(IL-4) (Fig. 1c). Further, only IntMs expressed CX3CR1 (Fig. 1c), supporting the idea that IntMs are derived from monocytes, while AlvMs at steady-state are resident cells[12, 18]. To verify that AlvMs reside in airways and IntMs in lung tissue, we administered CD45-PE antibodies intranasally (i.n.) and CD45-FITC antibodies intravenously (i.v.) prior to lung processing, to discriminate CD45-PE$^+$ airway macrophages from CD45-FITC$^+$ blood monocytes and tissue CD45-PE-FITC$^-$ tissue macrophages[22]. This approach indicated that AlvMs (defined throughout this study as MerTK$^+$CD64$^+$CD11b$^-$Siglec-F$^+$) were predominantly found in the airways, and IntMs (defined throughout this study as MerTK$^+$CD64$^+$CD11b$^+$Siglec-F$^-$) within the lung tissue (Fig. 1d), demonstrating that refined flow cytometry could discriminate between AlvM and IntM subsets.

Next, we investigated whether lung AlvMs and IntMs were functionally similar to macrophages in other tissues following systemic (intraperitoneal, i.p.) administration of recombinant IL-4 complexed with mAb to IL-4 (IL-4c), which extends the bioactive half-life of the cytokine and induces type 2 inflammation in C57BL/6 and BALB/c mice[4, 5]. PECMs underwent rapid expansion by day 4 after i.p. IL-4c injection on day 0 and day 2 (Fig. 1e)[4, 5], while AlvMs and IntMs were markedly less responsive to IL-4c, with no measurable increase in numbers of either population (Fig. 1e). Additionally, PECMs from IL-4c injected mice had elevated expression of markers of M(IL-4) activation (RELMα) and proliferation (Ki67 and EdU) (Fig. 1f and Supplementary Fig. 1b)[4]. AlvMs did not upregulate RELMα, Ki67 or EdU in response to IL-4c, whilst IntMs expressed intermediate levels of RELMα and Ki67 in comparison to PECMs (Fig. 1f and Supplementary Fig. 1b). Similar observations were made in BALB/c mice (data not shown). AlvMs and IntMs had lower responsiveness to systemic IL-4c compared to MerTK$^+$CD64$^+$CD11b$^+$ liver, colon or pleural cavity (PLEC) macrophages, which responded similarly to PECMs (Fig. 1g and Supplementary Fig. 1c). Together, this indicated that hypo-responsiveness to IL-4c was a feature of lung AlvMs and IntMs, and was particularly evident in AlvMs.

AlvMs express functional IL-4 receptor

Next we assessed whether AlvMs had reduced expression of IL-4 receptor (IL-4R) compared to IntMs and PECMs[4]. AlvM IL-4Rα expression was similar to that of IntMs and PECMs, and was not significantly affected by i.p. IL-4c (Fig. 2a). In addition, IL-4 was detected in BAL fluid

with similar dynamics as in peritoneal washes (Fig. 2b), indicating that i.p. injected IL-4c could reach the airways. To further address whether AlvM responsiveness to IL-4c depended on route of administration, we administered a range of concentrations of IL-4c i.n. (0.05 µg, 0.5 µg or 5 µg), with the lowest dose typical of that detected in airways during type 2 inflammation. Although IntMs significantly upregulated RELMα in response to i.n. IL-4c compared to PBS (Fig. 2c), AlvMs did not do so, even at the highest IL-4c dose (Fig. 2c). These observations indicated that lack of M(IL-4) activation was a characteristic feature of AlvMs, irrespective of IL-4c delivery route.

To investigate whether the lack of IL-4c responsiveness in AlvMs was due to impaired signalling, we measured expression of phosphorylated STAT6 (p-STAT6), a key transcription factor downstream of IL-4Rα engagement[2]. Both AlvMs after IL-4 i.n., and PECMs after IL-4 i.p., had increased p-STAT6 expression compared to PBS controls which was not evident in *Il4ra*$^{-/-}$ mice (Fig. 2d). In addition, AlvMs had high basal expression of p-STAT6, Ym1, pAkt T308 (mTORC1) and pAkt S473 (mTORC2) compared to PECMs, which was also evident in *Il4ra*$^{-/-}$ mice (Fig. 2d and Supplementary Fig. 2). This showed that AlvMs displayed IL-4Rα-independent 'tonic' STAT6 and mTORC signalling in the steady state, and could respond to i.n. IL-4 through STAT6 phosphorylation.

AlvMs show limited M(IL-4) activation during helminth infection

To assess whether differential activation of AlvMs and IntMs was apparent in settings other than IL-4c injection, we infected C57BL/6 mice s.c. with the parasite *Nippostrongylus brasiliensis*, against which a type 2 response is essential for tissue repair as larvae migrate through the lung, and for clearance of adult worms from the intestines[23]. As expected, a type 2 response, with eosinophilia and increased levels of RELMα in BAL fluid, was detected after infection, compared to naïve mice (Fig. 3a,b). As infection progressed from day 2 to day 7, IntMs increased in numbers (Fig. 3c,d) and upregulated the M(IL-4) markers RELMα, Arginase-1 and Ym1 markedly more than AlvMs (Fig. 3e and Supplementary Fig. 3b,c). Further, IntMs expressed higher levels of Ki67 than AlvMs by day 7 post-infection (Fig. 3e and Supplementary Fig. 3b), indicating that AlvMs did not acquire a clear M(IL-4) phenotype during infection. These observations contradict previous reports of AlvM M(IL-4) activation during type-2 inflammation[6, 7, 8, 9, 23]. However, these previous studies have generally defined AlvMs as CD11c^{+}Siglec-F^{+} (Supplementary Fig. 4a). Reliance on CD11c and Siglec-F to identify AlvMs could result in the inclusion of RELMα^{+} IntMs and eosinophils, particularly in inflamed mice (Supplementary Fig. 4a-d). Furthermore, use of scatter parameters in flow cytometry to exclude eosinophils could remove macrophages with similar granularity and SiglecF, CD11b or CD11c expression (Supplementary Fig. 4e,f). Using refined flow cytometry, we have demonstrated that M(IL-4) activation of AlvMs was impaired in comparison to IntMs during *N. brasiliensis* infection.

The pulmonary niche regulates AlvM responsiveness to IL-4

The lung environment is a unique site that shapes macrophage development[24], with environmental signals vital for directing this process[19]. Further, upon removal from tissues, macrophages in culture display fundamentally altered gene expression[25, 26]. Consistent with reports that AlvMs from mice and humans can respond to IL-4 *in vitro*[2], AlvMs isolated from the lungs of C57BL/6 mice significantly up-regulated expression of *Retnla* (encoding RELMα) and *Arg-1* after 48h in culture with IL-4, while expression of *Chil3* (encoding Ym1) was elevated after 12h compared to PBS controls (Fig. 4a). We next addressed whether the airway environment limited the ability of AlvMs to undergo M(IL-4) polarization. We transferred CD45.2$^+$ PECMs, which responded strongly to IL-4 *in vivo* (Fig. 1), i.n. into naïve CD45.1$^+$ mice, followed by administration of IL-4c i.p. Donor CD45.2$^+$ PECMs were detected in the lungs of recipient mice at day 5 post-transfer (Fig. 4b). However, PECMs transferred i.n. displayed an activation profile similar to that of resident AlvMs, failing to up-regulate RELMα and Ki67 in response to i.p. IL-4c administration compared to recipient PECMs (Fig. 4c). IL-4Rα expression on transferred CD45.2$^+$ PECMs was similar to recipient PECMs (Fig. 4d), suggesting that the impaired response of i.n. PECMs to IL-4 was not due to altered IL-4Rα expression.

Interaction between the inhibitory receptor CD200R and its ligand CD200 has been described as a dominant negative regulator of AlvM activation in non-type 2 settings[16]. Although expression of CD200R was highest on AlvMs compared to IntMs (Supplementary Fig. 5a), we observed no significant difference in numbers of AlvMs or IntMs, or their expression of RELMα or Ki67, following i.p. IL-4c injection of *Cd200r1*$^{-/-}$ mice (Supplementary Fig. 5b), indicating that AlvM hypo-responsiveness to IL-4 was independent of regulatory CD200-CD200R interactions.

In addition to immune mechanisms, macrophage responses at barrier sites may be modulated by airway components such as surfactant or mucus. SP-A and SP-D are abundant in the lower airways[27] and have been implicated in promotion of type 2 inflammation and M(IL-4) activation of AlvMs during helminth infection[21, 28], while mucus is a major regulator of responses in lung and airway macrophages[29]. IL-4c increased expression of the dominant pulmonary mucin Muc5b in airway epithelial cells compared to PBS-treated mice (Supplementary Fig. 5c). However, IntMs and AlvMs in *Muc5b*$^{-/-}$ and *Sftpd*$^{-/-}$ mice responded to IL-4c similarly to wild-type mice (Supplementary Fig. 5d,e), indicating that neither Muc5b nor SP-D were dominant factors in limiting the ability of lung AlvMs to undergo M(IL-4) polarization.

The airways host a wide diversity of commensals that could influence macrophage responses and are proposed to be key in regulating pulmonary allergic inflammation[30]. Further, gut microbe-derived short chain fatty acids are able to systemically regulate type 2 responses in the lung[31]. To test the involvement of commensals in regulating IL-4 responsiveness of AlvMs, we compared expression of RELMα and Ki67 in gnotobiotic (germ free (GF)) mice and conventionally-housed (specific pathogen free (SPF)) mice following i.p. IL-4c administration. RELMα and Ki67 expression on AlvMs, IntMs or PECMs was similar in IL-4c-treated GF and SPF mice (Fig. 4e), indicating that neither commensals nor their metabolites were involved in regulation of IL-4

responsiveness in any of these macrophage types. Together, these data indicated that the lung environment controlled AlvM responsiveness to IL-4**,** but this was independent of the microbiota, Muc5b or SP-D.

AlvMs and PECMs have distinct metabolic gene profiles

To address which factors might determine the lack of AlvM responsiveness to IL-4 *in vivo*, we next performed genome-wide mRNA profiling of AlvMs, IntMs and PECMs isolated from C57BL/6 mice injected i.p. with IL-4c or PBS. IL-4c induced a marked alteration of PECM gene expression, with 2074 transcripts significantly up- or down-regulated compared to PECMs from PBS-injected mice, including up-regulation of core M(IL-4) genes such as *Chil3*, *Retnla*, *Arg1* and *Mrc1* (encoding mannose receptor) (Fig. 5a,b and Supplementary Tables 1,2). IntMs in IL-4c-treated mice significantly up- or down-regulated 107 transcripts relative to IntMs from PBS-injected mice, including up-regulation of *Chil3* and *Retnla*, but not *Arg1* or *Mrc1* (Fig. 5a,b and Supplementary Tables 3,4), while IL-4c did not significantly up-regulate any of the core transcripts previously associated with M(IL-4) responsiveness in AlvMs, having almost no measurable impact on mRNA expression, with only 2 genes significantly down-regulated compared to AlvMs from PBS-treated mice: *Mipol1*, a putative tumor suppressor[32] and *Gnpat*, which is involved in lipid metabolism[33] (Fig. 5a,b and Supplementary Table 5). This indicated that AlvMs were broadly unresponsive to IL-4 *in vivo*. Further, AlvMs in PBS-treated mice had high basal expression of *Chil3* and *Mrc1* mRNA (Fig. 5b), consistent with high expression of Ym1 protein in steady-state AlvMs (Fig. 1c) and indicating that these markers are not suitable for M(IL-4) assessment in AlvMs. Kyoto Encyclopedia of Genes and Genomes (KEGG) analysis showed that the major pathways altered in PECMs by IL-4c included those involved in proliferation and metabolic processes (Supplementary Fig. 6a). However, few of these pathways were altered in response to IL-4c in AlvMs or IntMs (Supplementary Fig. 6b,c).

Next, we directly compared transcript expression in AlvMs and PECMs from IL-4c-treated mice. This analysis indicated substantially different gene expression profiles between the two macrophage populations (Fig. 5c and Supplementary Tables 6,7). In particular, pathways associated with glycolysis were impaired, while those associated with lipid metabolism and differentiation, such as PPAR and TGF-β, were elevated in AlvMs compared to PECMs (Fig. 5d,e and Supplementary Fig. 6d). These observations suggested that AlvM hypo-responsiveness to IL-4 may be due to impaired glycolysis, and confirmed previous reports that lung macrophages have a distinctive metabolic state compared to macrophages in other tissues[13].

Impaired glycolysis limits AlvM IL-4 responsiveness *in vivo*

To investigate whether AlvMs had reduced glycolytic ability compared to PECMs we analyzed changes in extracellular acidification rates (ECAR), a measure of glycolytic activity through detection of lactic acid as an end product of glucose metabolism[34], in AlvMs and PECMs

from naïve C57BL/6 mice. AlvMs exhibited significantly impaired glycolysis (reduced ECAR following glucose addition) and glycolytic reserve and capacity (defined as the ability to upregulate aerobic glycolysis) compared to PECMs (Fig. 6a). Analysis of oxygen consumption rates (OCR) showed that AlvMs also displayed reduced respiratory capacity (oxidative phosphorylation (OXPHOS)) compared to PECMs (Supplementary Fig. 7a). Culture of freshly isolated AlvMs or PECMs with the glucose analogue 2-NBDG, to measure uptake potential and glycolytic activity, showed that AlvMs acquired less 2-NBDG than PECMs, even when co-cultured at a 1:1 ratio with PECMs (Fig. 6b). Further, both $CD45.2^+$ PECMs transferred i.n. into $CD45.1^+$ mice and resident $CD45.1^+$ AlvMs had a reduced ability to acquire 2-NBDG *in vivo* following i.p. IL-4c, when compared to resident $CD45.1^+$ PECMs (Fig. 6c). Together, these observations indicated that the lung environment impaired the ability of AlvMs to both take up and utilize glucose.

However, AlvMs isolated from the lung and cultured for 48h *in vitro* showed increased expression of *Slc2a6* and *Eno1*, genes involved in glucose uptake and glycolysis (Fig. 6d), indicating that *ex vivo* culture of AlvMs enhanced their glycolytic ability. Next, we addressed whether glucose or fatty acid utilization was required for AlvMs to regain IL-4 responsiveness *in vitro*. The ability of cultured AlvMs to upregulate *Retnla*, *Arg1* and *Chil3 in vitro* in response to IL-4 was markedly inhibited by 2-deoxyglucose (2-DG), a competitive glucose inhibitor, compared to culture with IL-4 alone (Fig. 6e), but not significantly affected by addition of etomoxir, an inhibitor of fatty acid oxidation (FAO) (Supplementary Fig 7b). Similarly, even though AlvMs had high expression of genes associated with the TGF-β pathway (Fig. 5d), and addition of TGF-β reduced expression of IL-4-induced *Retnla* in cultured AlvMs (Supplementary Fig. 7c), it had no significant effect on *Chil3* expression, and increased *Arg-1* expression, suggesting that TGF-β was not a vital factor in limiting AlvM IL-4 responsiveness. Together, these data indicated that the lung environment regulated AlvM M(IL-4) activation through modulation of their metabolism.

Discussion

Here we have shown that AlvMs were hypo-responsive to type 2 inflammation mediated by IL-4c injection or helminth infection. This lack of responsiveness was conferred by the lung environment and impacted AlvM metabolic activity and ability to both take up and metabolize glucose. Removal of AlvMs from the lung reversed this metabolic constraint, enabling their M(IL-4) activation.

Although numerous studies have reported that pulmonary macrophages upregulate M(IL-4) markers, they either did not unequivocally distinguish between AlvMs and IntMs in their analyses, or relied on IL-4 stimulation of macrophages *ex vivo,* or used M(IL-4) markers that are already highly expressed by AlvMs at steady-state[6, 7, 8, 9, 20, 21]. Our results suggest that such work may require re-assessment to precisely identify which macrophage populations respond to IL-4 *in vivo.* Our data indicate that IntMs will be the major macrophage sub-population to respond in pulmonary type 2 inflammatory settings. This distinction is likely to be important for accurate understanding of the pathogenesis of pulmonary type 2 disease, given that M(IL-4) macrophages have been implicated in wound repair during type 2 inflammation[23, 35]. Thus, we would speculate that IntMs will play a more important role than AlvMs in processes such as resolving tissue damage in the lung, due to their greater ability to respond to IL-4.

Although negative regulation of macrophage activation is a well described feature of the lung, and is thought to be vital to restrict over-exuberant responses against inhaled material, viral or bacterial infection[1], how pulmonary M(IL-4) responses are regulated is currently poorly understood. While we have not identified which specific components of the pulmonary environment restricted AlvM activation by IL-4, we have shown that this was independent of Muc5b, SP-D and commensals or their metabolite products, all of which are features of the lung that have previously been implicated in modulating pulmonary macrophage responses to bacteria, helminth infection and allergic airway inflammation[28, 29, 31].

Metabolism is a key determinant of immune cell function and is central in governing how macrophages respond to a variety of signals, including type 1 and type 2 cytokines[34, 36]. The majority of studies so far have profiled metabolic responses in bone marrow-derived macrophages *in vitro*[37], and have not addressed how tissue environments alter macrophage metabolism and function *in vivo*. From such work, it has been proposed that type 2 cytokines promote amino acid and lipid metabolism (including FAO) feeding into OXPHOS, whereas glycolysis is more associated with type 1 macrophage polarization[34, 37, 38, 39]. We found that AlvMs had a distinctive metabolic state compared to PECMs, with elevated expression of genes associated with PPAR-γ and lipid metabolism, a profile that would be expected to enhance FAO, OXPHOS and M(IL-4) activation[34, 37, 38]. However, defective glycolytic ability rendered AlvMs hypo-responsive to IL-4, consistent with recent observations that glycolysis can mediate macrophage responses to IL-4[40, 41], and with studies linking altered metabolic state with AlvM ability to respond to *Mycobacterium tuberculosis*[42]. Our demonstration that the lung environment controls macrophage metabolism

during type 2 inflammation, together with recent evidence that metabolism also regulates DC control of allergic airway inflammation[43], suggests caution in interpreting metabolic data generated from model macrophages or DCs in culture. Our data also imply that the distinctive metabolic profile of AlvMs may be directly linked to negative regulation of their activation and function at steady-state and during inflammation[1].

One factor to consider in how the lung may affect AlvM activation is amounts of metabolic substrates, including glucose, present in airways. Glucose levels in air surface liquid, which covers the airway epithelium, are 12.5-fold lower than in blood[44]. Such low glucose concentrations, maintained through highly-effective epithelial cell glucose transport[45], appear vital to prevent bacterial outgrowth in airways[44, 46]. Elevated glucose is found in patient sputum during chronic obstructive pulmonary disease[47], while glucose levels and glucose metabolism rise in the lung during asthma[48, 49]. Together with our data, this leads to the intriguing hypothesis that glucose availability and/or utilization could be exploited to therapeutically modify pulmonary disease.

We showed that AlvMs removed from the airways regained ability to respond to IL-4 *in vitro*, while PECMs transferred into the airways lost IL-4 responsiveness. The stark difference between AlvM ability to respond to IL-4 *in vitro* and *in vivo* resonates with the reported transformation of microglial transcriptional identity when removed from the brain[25, 26], and cautions against reliance on AlvMs *in vitro* for functional studies. This may be particularly relevant for human AlvMs, given current experimental dependence on their culture *ex vivo,* and highlights the need for development of innovative approaches to better assess human AlvM function *in vitro*. Similarly, identification of markers for human macrophage subpopulations and their M(IL-4) activation is urgently needed. The current revolution in single cell sequencing for definition of cellular networks suggests that this approach applied to human AlvMs should be illuminating. In both human and murine type 2 inflammation, it will also be important to understand how monocytes recruited to the lung differentiate and influence airway or tissue macrophages, as resident AlvMs can be replaced by regulatory monocytes during viral infection[50]. Our data suggests that the airway environment will play a key role in influencing activation and function of AlvMs during type 2 inflammation, irrespective of their origin.

More broadly, this work illustrates the pivotal role of the tissue environment in the regulation of metabolic activity and ability to respond to type 2 cytokines in AlvMs, a principle that will likely be relevant in diverse tissue and disease settings. Local differences in substrate availability, and alterations of such during inflammation, may provide an elegant metabolic mechanism to modulate the activation and function of macrophages and other immune cells in a tissue-specific manner in health and in disease.

Acknowledgements

We thank members of the MCCIR and MacDonald laboratory (University of Manchester) for scientific discussions and some experimental assistance, J. Allen (University of Manchester) for critical reading of the manuscript, the University of Manchester Single Cell Facility for flow cytometry, cell sorting and ImageStream, K. Couper and J. Grainger (University of Manchester) for provision of Pep3 and CX3CR1eGFP mice and M. Travis for providing recombinant TGF-β. This research was supported by a MCCIR PhD studentship (F.R.S.), the Medical Research Council (MR/P026907/1, H.C. and J.M.) the National Institutes of Health (HL080396 and HL130938, C.M.E.), the Wellcome Trust Institutional Strategic Support Fund [105610] (R.K.G., D.J.T. and M.Z.K.), Medical Research Foundation UK joint funding with Asthma UK (MRFAUK-2015-302, T.E.S.), BBSRC studentship (C.S.), a University of Manchester Dean's Prize Early Career Research Fellowship (P.C.C.), Springboard Award (Academy of Medical Sciences, SBF002/1076, P.C.C.) and MCCIR core funding (A.S.M. and T.H.). This work was also made possible through use of the Manchester Gnotobiotic Facility that was established with the support of the Wellcome Trust [097820/Z/11/B], using founder mice obtained from the Clean Mouse Facility, University of Bern, Switzerland. The Bioimaging Facility microscopes used in this study were purchased with grants from BBSRC, Wellcome Trust and the University of Manchester Strategic Fund.

Authors contributions

Conceptualization, P.C.C, A.S.M.; Methodology, F.R.S., S.L.B., M.Z.K., L.C., M.C., G.H., A.C.I., P.C.C.; Investigation, F.R.S., S.L.B., M.Z.K., L.C., C.S., M.C., G.H., T.E.S., A.C.I., P.C.C.; Resources, H.C., J.M., C.M.E., T.E.S., D.J.T., R.K.G., D.M.C., T.H., A.S.M.; Writing – Original Draft, F.R.S. P.C.C., A.S.M.; Writing – Review & Editing, F.R.S., S.L.B., C.M.E., A.C.I., D.J.T., R.K.G., D.M.C., T.H., P.C.C., A.S.M.; Funding Acquisition, D.J.T, R.K.G., D.M.C., T.H., P.C.C., A.S.M.

Competing interests

The authors declare no competing interests.

Figure legends

Fig 1. Alveolar macrophages are unresponsive to IL-4. a, Flow cytometry plots identifying AlvMs and IntMs from BAL fluid or lung tissue of naïve mice. Data representative of 8 independent experiments. **b**, Imaging cytometry of AlvMs and IntMs from lung tissue of naïve mice (scale bar: 10μm). **c**, Histograms of expression of F4/80, CD11c, Ym1 and eGFP by *Cx3cr1*$^{eGFP/+}$ mice by IntMs and AlvMs from lung tissue of naïve mice. **d**, Flow cytometry plots of AlvMs, IntMs and monocytes from lung tissue of naïve mice following CD45 i.n. and i.v. administration. b-d, representative data from 3 independent experiments. **e**, Numbers of lung tissue AlvMs and IntMs, or PECMs, on d4 following i.p. PBS or IL-4c administration on d0 and d2. Data representative of 7-9 experiments, n=26 (AlvM PBS, AlvM IL-4c, IntM PBS, IntM IL-4c), n=18 (PECM PBS), n=13 (PECM IL-4c) mice per group. **f**, RELMα and Ki67 expression, or EdU incorporation, by lung tissue AlvMs and IntMs, or PECMs, on d4 following i.p. PBS or IL-4c administration on d0 and d2, and EdU injection i.p. 3h before tissue collection. Graphs show individual replicate mice, data pooled from 5-9 independent experiments, RELMα: n=29 (AlvM PBS, AlvM IL-4c, IntM PBS, IntM IL-4c), n=24 (PECM PBS), n=23 (PECM IL-4c) mice per group. Ki67: n=24 (AlvM PBS, IntM PBS), n=23 (AlvM IL-4c, IntM IL-4c), n=20 (PECM PBS, PECM IL-4c) mice per group. EdU: n=22 (AlvM PBS, AlvM IL-4c, IntM PBS), n=23 (IntM IL-4c), n=14 (PECM PBS), n=17 (PECM IL-4c) mice per group. **g**, Percentage of RELMα^{+} PECMs, PLECMs, Kupffer cells, IntMs and AlvMs on d4 following i.p. PBS or IL-4c administration on d0 and d2. Data representative of 2-5 independent experiments, n=5 (PBS PECMs, Kupffer cells, IntMs and AlvMs), n=4 (IL-4c PLECMs), n=3 (PBS PLECMs, colon Ms and IL-4c PECMs, Kupffer cells, colon Ms, IntMs, AlvMs) mice per group. e-g, data analysed by two-way analysis of variance (ANOVA) with Tukey's post-test for multiple comparisons, displayed as mean ± SEM, **P*<0.05, ****P*<0.001 and *****P*<0.0001.

Fig. 2. Alveolar macrophages are less responsive than interstitial macrophages to IL-4c administered directly into the airways. a, IL-4Rα expression by AlvMs, IntMs or PECMs from mice injected with PBS or IL-4c i.p. on d0 and d2, and lung tissue and PEC collected on d4. Histograms representative of 2 independent experiments. **b**, ELISA of IL-4 levels in BAL or PEC fluids 6h, 12h, 24h or 48h after i.p. injection of PBS or IL-4c. Data representative of 2 independent experiments, n=2 (PBS, 24h and 48h), n=3 (6h and 12h) mice per group. **c**, Flow cytometry plots of RELMα expression in lung tissue AlvMs and IntMs on d4 following i.n. PBS or IL-4c administration on d0 and d2 (left) and quantification of the percentage of RELMα^{+} cells (right). Data representative of 3 independent experiments, n=2 (5μg AlvM), n=3 (AlvM: PBS, 0.05 & 0.5μg. IntM: PBS, 0.05, 0.5 & 5μg) mice per group. **d**, Histograms of pSTAT6 levels in lung tissue AlvMs or PECMs 15 min after PBS or rIL-4 administered i.n. or i.p. to WT or *Il4ra*$^{-/-}$ mice (left), and quantification of AlvM and PECM pSTAT6 expression (right). Data representative of 2 independent experiments, n=3 mice per group. Data analysed by one-way analysis of variance

(ANOVA) with Tukey's post-test for multiple comparisons, displayed as mean ± SEM, *P<0.05, ***P<0.001 and ****P<0.0001.

Fig. 3. Alveolar macrophages are less responsive than interstitial macrophages during helminth infection. a, Eosinophil numbers from lung tissue of naïve mice or on d2, d4 and d7 following infection s.c. with 500 L3 *N. brasiliensis* larvae. Graphs show individual replicate mice, data pooled from 4 independent experiments, n=18 (naïve), n=17 (d2), n=9 (d4), n=5 (d7) mice per group. **b**, ELISA of RELMα levels in BAL fluid from naïve or infected mice. Data pooled from 2 independent experiments, n=8 (naïve), n=7 (d2), n=4 (d4), n=3 (d7) mice per group. **c**, Numbers of lung tissue AlvMs and IntMs from naïve or infected mice. Data pooled from 4 independent experiments, n=18 (naïve), n=17 (d2), n=9 (d4), n=8 (d7) mice per group. **d**, Flow cytometry plots identifying lung tissue AlvMs and IntMs from naïve or infected mice. Data representative of 4 independent experiments. **e**, Quantification of the percentage of RELMα$^+$ and Ki67$^+$ lung tissue AlvMs and IntMs from naïve or infected mice. Data pooled from 4 independent experiments, n=18 (Naïve RELMα), n=17 (d2 RELMα), n=9 (d4 RELMα), n=8 (d7 RELMα), n=13 (Naïve Ki67), n=12 (d2 Ki67), n=5 (d4 Ki67), n=3 (d7 Ki67) mice per group. Data analysed by one-way analysis of variance (ANOVA) with Tukey's post-test for multiple comparisons, displayed as mean ± SEM, *P<0.05, **P<0.01, ***P<0.001 and ****P<0.0001.

Fig. 4. The pulmonary niche regulates alveolar macrophage responsiveness to IL-4 independently of host commensals. a, mRNA expression by qPCR of lung tissue AlvMs from naïve mice following culture for 12h, 24h or 48h in media alone or with rIL-4 (20 ng/ml). A.U. arbitrary units. Data representative of 4 independent experiments, n=2 (media), n=3 (rIL-4) wells per group, each group pooled cells from 8 mice. **b - e**, Donor (CD45.2$^+$) and host (CD45.1$^+$) macrophage populations identified by flow cytometry in lung tissue or PEC from host mice on d5 after i.n. PBS or donor PECM transfer on d0, then injection with IL-4c i.p. on d1 and d3. **b**, Flow cytometry plots identifying donor PECMs in host lung tissue. Data representative of 4 independent experiments**. c**, Quantification of the percentage of RELMα$^+$ and Ki67$^+$ host and donor macrophages isolated from host lung tissue or PEC. Data representative of 4 independent experiments, n=6 mice per group. **d**, IL-4Rα expression by donor PECMs isolated from host lung tissue. Histogram representative of 2 independent experiments**. e**, RELMα and Ki67 expression by lung tissue AlvMs and IntMs, or PECMs, from specific pathogen free (SPF) or Germ Free (GF) mice on d4 following i.p. PBS or IL-4c administration on d0 and d2. Data representative of 3 independent experiments, n=3 mice per group. Data analysed by one-way analysis of variance (ANOVA) with Tukey's post-test for multiple comparisons, displayed as mean ± SEM, **P<0.01, ***P<0.001 and ****P<0.0001.

Fig. 5. Alveolar and peritoneal macrophages display dramatically different metabolic gene profiles. a, mRNA expression profiles (volcano plots) as determined by RNA-seq of PECMs, IntMs or AlvMs isolated from lung tissue or PEC by flow cytometry on d4 following i.p. PBS or IL-4c administration on d0 and d2. Dashed lines represent $P<0.01$, and ± 2-fold change, IL-4c relative to PBS. **b**, Heatmaps of selected mRNA transcripts of genes that have been previously described as M(IL-4) markers, *indicates significance between IL-4c vs. PBS of at least p<0.01.**c**, mRNA expression profile (volcano plot) of AlvMs vs. PECMs isolated from IL-4c injected mice. Dashed lines represent $P<0.01$, and ± 2-fold change. **d**, Selected pathways from KEGG analysis (Supplementary Fig. 6) of significantly altered mRNA transcripts from (**c**), black lines represent $P<0.05$. **e**, Relative transcript expression by AlvMs vs. PECMs from IL-4c injected mice that were significantly altered ($P<0.01$, log2 normalized intensity), as identified from the glycolysis pathway by network analysis (several genes displayed more than one altered transcript variant), n=2 (PECM PBS, PECM IL-4c, AlvM PBS, IntM PBS, IntM IL-4c), n=3 (AlvM IL-4c) separate biological replicates, each replicate pooled cells from 3-5 mice.

Fig. 6. Impaired uptake and utilization of glucose renders alveolar macrophages unresponsive to IL-4.

a, ECAR of AlvMs and PECMs isolated from lung tissue or PEC of naïve mice by flow cytometry, at baseline and after sequential treatment (vertical lines) with glucose, oligomycin (Oligo) or 2-Deoxy-D-glucose (2-DG) to measure glycolysis, glycolytic reserve and glycolytic capacity. Data representative of 4 independent experiments, n=6 (AlvM), n=10 (PECM) glycolytic stress test profile, n=6 (AlvM) glycolysis, glycolytic capacity and glycolytic reserve, n=10 (PECM) glycolysis, glycolytic capacity, n=9 (PECM) glycolytic reserve, wells per group, each group pooled cells from 8 mice. **b**, Flow cytometry plots of 2-NBDG uptake *in vitro* by BAL AlvMs or PECMs from naïve mice cultured separately or at a 50:50 mix for 20 min with fluorescently labelled 2-NBDG. 2-NBDG uptake *in vivo* by donor ($CD45.2^+$) and host ($CD45.1^+$) macrophage populations identified by flow cytometry in lung tissue or PEC from host mice on d5 after i.n. PBS or donor PECM transfer on d0, administration of IL-4c i.p. on d1 and d3, and i.p. injection of fluorescently labelled 2-NBDG 20 min prior to lung tissue and PEC collection. Data representative of 2 independent experiments, n=6 mice per group. **d**, mRNA expression by qPCR of lung tissue AlvMs from naïve mice cultured for 12h, 24h or 48h in media alone. A.U. arbitrary units. Data representative of 6 (Eno1) or 5 (Slc2a6) independent experiments, n=3 (Eno1), n=2 (Slc2a6) wells per group, each group pooled cells from 6-8 mice. **e**, mRNA expression by qPCR of lung tissue AlvMs from naïve mice cultured for 48h in media alone, or with rIL-4 ± 2-DG. Data representative of 3 independent experiments, n=2 (media), n=3 (rIL-4), n=3 (rIL-4 + 2-DG) wells per group, each group pooled cells from 6-8 mice. Data analysed using unpaired *t* test (a) or a one way analysis of variance (ANOVA) with Tukey's post-test for multiple comparisons as indicated (b, c & e) or compared to 0h (d), displayed as mean ± SEM, *$P<0.05$, ***$P<0.001$ and ****$P<0.0001$.

502

References

1. Hussell, T. & Bell, T.J. Alveolar macrophages: plasticity in a tissue-specific context. *Nature reviews. Immunology* **14**, 81-93 (2014).
2. Van Dyken, S.J. & Locksley, R.M. Interleukin-4- and interleukin-13-mediated alternatively activated macrophages: roles in homeostasis and disease. *Annual review of immunology* **31**, 317-343 (2013).
3. Gundra, U.M. *et al.* Vitamin A mediates conversion of monocyte-derived macrophages into tissue-resident macrophages during alternative activation. *Nature immunology* **18**, 642-653 (2017).
4. Jenkins, S.J. *et al.* Local macrophage proliferation, rather than recruitment from the blood, is a signature of TH2 inflammation. *Science* **332**, 1284-1288 (2011).
5. Jenkins, S.J. *et al.* IL-4 directly signals tissue-resident macrophages to proliferate beyond homeostatic levels controlled by CSF-1. *The Journal of experimental medicine* **210**, 2477-2491 (2013).
6. Bhatia, S. *et al.* Rapid host defense against Aspergillus fumigatus involves alveolar macrophages with a predominance of alternatively activated phenotype. *PloS one* **6**, e15943 (2011).
7. Dai, S., Rajaram, M.V., Curry, H.M., Leander, R. & Schlesinger, L.S. Correction: Fine Tuning Inflammation at the Front Door: Macrophage Complement Receptor 3-mediates Phagocytosis and Immune Suppression for Francisella tularensis. *PLoS pathogens* **12**, e1005504 (2016).
8. Robbe, P. *et al.* Distinct macrophage phenotypes in allergic and nonallergic lung inflammation. *Am J Physiol Lung Cell Mol Physiol* **308**, L358-367 (2015).
9. Reece, J.J., Siracusa, M.C. & Scott, A.L. Innate immune responses to lung-stage helminth infection induce alternatively activated alveolar macrophages. *Infection and immunity* **74**, 4970-4981 (2006).
10. Roberts, A.W. *et al.* Tissue-Resident Macrophages Are Locally Programmed for Silent Clearance of Apoptotic Cells. *Immunity* **47**, 913-927 e916 (2017).
11. Guilliams, M. *et al.* Alveolar macrophages develop from fetal monocytes that differentiate into long-lived cells in the first week of life via GM-CSF. *The Journal of experimental medicine* **210**, 1977-1992 (2013).
12. Ginhoux, F. & Guilliams, M. Tissue-Resident Macrophage Ontogeny and Homeostasis. *Immunity* **44**, 439-449 (2016).
13. Schneider, C. *et al.* Induction of the nuclear receptor PPAR-gamma by the cytokine GM-CSF is critical for the differentiation of fetal monocytes into alveolar macrophages. *Nature immunology* **15**, 1026-1037 (2014).
14. Yu, X. *et al.* The Cytokine TGF-beta Promotes the Development and Homeostasis of Alveolar Macrophages. *Immunity* **47**, 903-912 e904 (2017).
15. Westphalen, K. *et al.* Sessile alveolar macrophages communicate with alveolar epithelium to modulate immunity. *Nature* **506**, 503-506 (2014).
16. Snelgrove, R.J. *et al.* A critical function for CD200 in lung immune homeostasis and the severity of influenza infection. *Nature immunology* **9**, 1074-1083 (2008).
17. Gautier, E.L. *et al.* Gene-expression profiles and transcriptional regulatory pathways that underlie the identity and diversity of mouse tissue macrophages. *Nature immunology* **13**, 1118-1128 (2012).
18. Gibbings, S.L. *et al.* Three Unique Interstitial Macrophages in the Murine Lung at Steady State. *Am J Respir Cell Mol Biol* (2017).
19. Guilliams, M. & Scott, C.L. Does niche competition determine the origin of tissue-resident macrophages? *Nature reviews. Immunology* **17**, 451-460 (2017).
20. Bosurgi, L. *et al.* Macrophage function in tissue repair and remodeling requires IL-4 or IL-13 with apoptotic cells. *Science* **356**, 1072-1076 (2017).
21. Minutti, C.M. *et al.* Local amplifiers of IL-4Ralpha-mediated macrophage activation promote repair in lung and liver. *Science* **356**, 1076-1080 (2017).
22. Wiesner, D.L., Smith, K.D., Kashem, S.W., Bohjanen, P.R. & Nielsen, K. Different Lymphocyte Populations Direct Dichotomous Eosinophil or Neutrophil Responses to Pulmonary Cryptococcus Infection. *Journal of immunology* **198**, 1627-1637 (2017).

23. Chen, F. *et al.* An essential role for TH2-type responses in limiting acute tissue damage during experimental helminth infection. *Nature medicine* **18**, 260-266 (2012).
24. Lavin, Y. *et al.* Tissue-resident macrophage enhancer landscapes are shaped by the local microenvironment. *Cell* **159**, 1312-1326 (2014).
25. Gosselin, D. *et al.* Environment drives selection and function of enhancers controlling tissue-specific macrophage identities. *Cell* **159**, 1327-1340 (2014).
26. Gosselin, D. *et al.* An environment-dependent transcriptional network specifies human microglia identity. *Science* **356** (2017).
27. Haczku, A. Protective role of the lung collectins surfactant protein A and surfactant protein D in airway inflammation. *J Allergy Clin Immunol* **122**, 861-879; quiz 880-861 (2008).
28. Thawer, S. *et al.* Surfactant Protein-D Is Essential for Immunity to Helminth Infection. *PLoS pathogens* **12**, e1005461 (2016).
29. Roy, M.G. *et al.* Muc5b is required for airway defence. *Nature* **505**, 412-416 (2014).
30. Gollwitzer, E.S. *et al.* Lung microbiota promotes tolerance to allergens in neonates via PD-L1. *Nature medicine* **20**, 642-647 (2014).
31. Trompette, A. *et al.* Gut microbiota metabolism of dietary fiber influences allergic airway disease and hematopoiesis. *Nature medicine* **20**, 159-166 (2014).
32. Cheung, A.K. *et al.* Chromosome 14 transfer and functional studies identify a candidate tumor suppressor gene, mirror image polydactyly 1, in nasopharyngeal carcinoma. *Proc Natl Acad Sci U S A* **106**, 14478-14483 (2009).
33. Rodemer, C. *et al.* Inactivation of ether lipid biosynthesis causes male infertility, defects in eye development and optic nerve hypoplasia in mice. *Hum Mol Genet* **12**, 1881-1895 (2003).
34. O'Neill, L.A. & Pearce, E.J. Immunometabolism governs dendritic cell and macrophage function. *The Journal of experimental medicine* **213**, 15-23 (2016).
35. Knipper, J.A. *et al.* Interleukin-4 Receptor alpha Signaling in Myeloid Cells Controls Collagen Fibril Assembly in Skin Repair. *Immunity* **43**, 803-816 (2015).
36. Ip, W.K.E., Hoshi, N., Shouval, D.S., Snapper, S. & Medzhitov, R. Anti-inflammatory effect of IL-10 mediated by metabolic reprogramming of macrophages. *Science* **356**, 513-519 (2017).
37. Van den Bossche, J., O'Neill, L.A. & Menon, D. Macrophage Immunometabolism: Where Are We (Going)? *Trends in immunology* **38**, 395-406 (2017).
38. Eming, S.A., Wynn, T.A. & Martin, P. Inflammation and metabolism in tissue repair and regeneration. *Science* **356**, 1026-1030 (2017).
39. Pelgrom, L.R. & Everts, B. Metabolic control of type 2 immunity. *European journal of immunology* **47**, 1266-1275 (2017).
40. Huang, S.C. *et al.* Metabolic Reprogramming Mediated by the mTORC2-IRF4 Signaling Axis Is Essential for Macrophage Alternative Activation. *Immunity* **45**, 817-830 (2016).
41. Jha, A.K. *et al.* Network integration of parallel metabolic and transcriptional data reveals metabolic modules that regulate macrophage polarization. *Immunity* **42**, 419-430 (2015).
42. Huang, L., Nazarova, E.V., Tan, S., Liu, Y. & Russell, D.G. Growth of Mycobacterium tuberculosis in vivo segregates with host macrophage metabolism and ontogeny. *The Journal of experimental medicine* (2018).
43. Sinclair, C. *et al.* mTOR regulates metabolic adaptation of APCs in the lung and controls the outcome of allergic inflammation. *Science* (2017).
44. Gill, S.K. *et al.* Increased airway glucose increases airway bacterial load in hyperglycaemia. *Sci Rep* **6**, 27636 (2016).
45. Garnett, J.P. *et al.* Proinflammatory mediators disrupt glucose homeostasis in airway surface liquid. *Journal of immunology* **189**, 373-380 (2012).
46. Baker, E.H. & Baines, D.L. Airway Glucose Homeostasis: A New Target in the Prevention and Treatment of Pulmonary Infection. *Chest* (2017).
47. Mallia, P. *et al.* Role of airway glucose in bacterial infections in patients with chronic obstructive pulmonary disease. *J Allergy Clin Immunol* **142**, 815-823 e816 (2018).
48. Ho, W.E. *et al.* Metabolomics reveals altered metabolic pathways in experimental asthma. *Am J Respir Cell Mol Biol* **48**, 204-211 (2013).
49. Ostroukhova, M. *et al.* The role of low-level lactate production in airway inflammation in asthma. *Am J Physiol Lung Cell Mol Physiol* **302**, L300-307 (2012).

50. Machiels, B. *et al.* A gammaherpesvirus provides protection against allergic asthma by inducing the replacement of resident alveolar macrophages with regulatory monocytes. *Nature immunology* **18**, 1310-1320 (2017).

Methods

Experimental animals

Cx3cr1$^{eGFP/+}$, *Cd200r1*$^{-/-}$, CD45.1^{+}, *Il4ra*$^{-/-}$, *Muc5b*$^{-/-}$ and *Sftpd*$^{-/-}$ were generated as described previously[16, 28, 29]. All were on a C57BL/6 background except *Il4ra*$^{-/-}$ which were BALB/c. C57BL/6 or BALB/c mice were purchased from Envigo. Mice were bred and maintained under specific pathogen free conditions at The University of Manchester. Germ free mice were from the University of Manchester Gnotobiotic Facility. All experiments were approved under a project license granted by the Home Office U.K., and by the University of Manchester Animal Welfare and Ethical Review Body, and performed in accordance with the United Kingdom Animals (Scientific Procedures) Act of 1986.

In vivo mouse models

IL-4 complex delivery in vivo: Long acting IL-4 complexes (IL-4c: IL-4/anti IL-4mAb) were prepared and used as previously described[4, 5]. Recombinant murine IL-4 (BioLegend) was combined with rat IgG1 anti-IL-4 mAb 11B11 (BioXcell) at a 1:5 molecular weight ratio[51]. Mice were injected i.p. with 5 µg of IL-4 (complexed to 11B11) or Dulbeccos PBS (PBS, Sigma) on d0 and d2. Alternatively 50 µl of PBS or varying doses of IL-4c (5 – 0.05 µg) was administered directly i.n. on d0 and d2. Tissues were collected on d4 post initial injection.

N. brasiliensis infection: WT mice were infected s.c. with 500 *N. brasiliensis* third-stage larvae and tissues collected d2, d4 and d7 post infection.

In both models, to assess cell proliferation mice were injected i.p. with 0.5mg 5-ethynyl-2´-deoxyuridine (EdU) (ThermoFisher) in 200 µl PBS 3h prior to harvest to label cells in S-phase of cell cycle as has previously been described[3]. This short window was chosen to provide an accurate readout of *in situ* cell proliferation at the tissue of interest, and avoid detection of cells that had recently proliferated elsewhere prior to recruitment.

Isolation of immune cells from the peritoneal cavity, bronchoalveolar lavage, lung, intestine and liver.

Following sacrifice, PEC or BAL cells were obtained by washing of the peritoneal cavity or lungs with PBS containing 2% FBS and 2mM EDTA (Sigma). Lungs were processed as previously described[52], incubated at 37°C for 40 min with 0.8 U/ml Liberase TL and 80 U/ml DNase I type VI in HBSS (all Sigma). The digestion was stopped with PBS containing 2% FBS (Sigma) and 2 mM EDTA (Sigma), with the resulting suspension then passed through a 70 µm cell strainer. In some cases, prior to collection, i.v. or i.n. instillation of fluorescently labeled anti-CD45 (clone: 30-F11) was used to distinguish between blood circulating (i.v. CD45 FITC^{+}), airway resident (i.n. CD45 PE^{+}) and tissue resident leukocytes (CD45 FITC^{-}PE^{-}), as described previously[22, 53]. Mononuclear cells from the intestine and liver were isolated as previously described[54, 55]. Erythrocytes were lysed using RBC lysis buffer (Sigma) and cells counted and processed for flow cytometry.

Flow cytometry and cell sorting

Equal numbers of cells were stained for each sample, washed with ice-cold PBS and stained with Zombie UV dye (@1:2000, BioLegend) for 10 min at room temperature. All samples were then blocked with 5 µg/ml αCD16/CD32 (2.4G2; BioLegend) in FACS buffer (PBS containing 2% FBS and 2mM EDTA) before staining for specified surface markers at 4°C for 25 minutes. For detection of intracellular molecules, following surface staining cells were fixed with 1% paraformaldehyde in PBS for 10 min at room temperature, and permeabilized with the Transcription factor staining kit (eBioscience) then stained with the relevant antibodes. If mice had been treated with EdU, cells were stained using the Click-iT Plus EdU Alexa Fluor 647 Flow Cytometry Assay Kit (Molecular Probes) using an adapted protocol for a final staining volume of 50µl. Samples were acquired using a 5 laser Fortessa with BD FACSDiva software and analyzed with FlowJo software (v9 and v10, Tree Star). Sorting of macrophage populations from the PEC (based on DAPI^{-}F4/80^{+}) and lung (DAPI^{-}, CD45^{+}MerTK^{+}CD64^{+} and CD11b^{+} IntMs or Siglec-F^{+} AlvMs) was performed using an Influx (BD Biosciences) using the 140 µm nozzle and 7.5 psi pressure, to a purity of ~95-99%. In some cases, myeloid cells were enriched prior to sorting by removal of lymphoid cells using Dynabeads (ThermoFisher) (biotinylated anti-CD3, CD19, B220, Ly6G, NK1.1, Ter119 and streptavidin-Dynabeads) according to the manufacturers instructions.

pSTAT6 and pAkt intracellular staining

To assess pSTAT6 and pAkt activation, 5µg rIL-4 was administered i.n. or i.p. 15 min prior to tissue collection. Cells from PEC or BAL washes were directly incubated with an equal volume of formalin (final concentration 2% formalin) for at least 10 mins at room temperature, resuspended in 500µl ice cold methanol at 4ºC for 10 min, washed twice with FACS buffer, then stained and acquired (as described above).

Intranasal transfer of PEC macrophages into the airways

PECMs were sorted as described above from CD45.2 mice. PBS, or 1 x 10^6 donor PECMs in PBS, were instilled into the airways of CD45.1 recipient mice via i.n. transfer. Mice were treated with IL-4c (as described above) and cells from the lungs were isolated and processed as described above. In some experiments, 100 µg FITC labelled 2-NBDG (Sigma), internalization of which measures glucose uptake potential and glycolytic activity [56], was injected (i.p.) 20 min prior to tissue collection.

***In vitro* culture of macrophages**

AlvMs or PECMs FACS isolated from naïve mice (as described above) were cultured in RPMI 1640 (containing 10% FBS, 1% PenStrep, 1% L-glutamine, all Sigma) for up to 48h at 37ºC. In some experiments, they were incubated with 50 µg/ml FITC labeled 2-NBDG (Sigma) for 20 min (either separately or a 50:50 mix of the two), or in the presence of rIL-4 (20 ng/ml) ± 1 mM 2-DG (Sigma), 200 µM etomoxir (Sigma) or recombinant human TGF-β (10 ng/ml) (Peprotech).

Imaging cytometry

Cells were stained and fixed (as described above) in ImageStream buffer (PBS containing 1% FBS and 2 mM EDTA). Data acquisition was performed on ImageStreamX (Amnis/EMD Millipore, Seattle, WA) equipped with 405, 488, 561, and 642 nm lasers. Single cells were discriminated from cell aggregates based on area and aspect ratio. In focus cells were selected based on high gradient RMS of the bright field image. Images of cells were acquired with a ×40 objective including bright field images (Channels 1 & 9; 420–480nm and 570-595nm), CD11b (Channel 2; 480-560nm), MerTK (Channel 3; 560–595nm), Siglec-F (Channel 4; 595-660nm), CD64 (Channel 6; 740-800nm), Zombie UV (Channel 7; 420-505nm) and CD45 (Channel 8; 505-570nm). All data analysis was performed using the IDEAS® software version 6.

Histology

Histological sections were prepared from lungs perfused with freshly prepared metha-carnoys solution (60% absolute methanol, 30% choroform, 10% acetic acid) and embedded in paraffin. 5 µM sections were subjected to immunohistochemical analysis for Muc5b (custom polyclonal antisera)[57]. Bound primary antibody was detected with goat anti-rabbit Alexa fluor 488. Images were captured using an Olympus BX51 upright microscope using a 20x /0.5 EC Plan-neofluar objective and captured using a Coolsnap ES camera (Photometrics) through MetaVue Software (Molecular Devices). Images were then processed and analyzed using ImageJ[58].

Enzyme linked immunosorbent assay (ELISA)

ELISAs to detect RELMα (PeproTech) and IL-4 (BioLegend) were performed on BAL or PEC fluid, as per manufacturers instructions.

RNA isolation, library construction and analysis

To generate RNA libraries of sorted macrophage populations, mice were exposed to PBS or IL-4c and two separate pooled biological replicates were generated for PECM PBS, PECM IL-4c, AlvM PBS, IntM PBS and IntM IL-4c groups while three separate pooled replicates were collected for the AlvM IL-4c group. Each pooled biological replicate was generated from cells isolated from 3 – 5 mice. After FACS sorting, each sample was lysed with RLT buffer (Qiagen) and RNA isolated with RNeasy microkits (Qiagen) according to the manufacturers instructions. Sample RNA integrity was confirmed using TapeStation (Agilent), with all samples showing RNA integrity numbers of ~8.8-10. RNA quality was assessed by Fragment Analyzer (Advanced Analytical Technologies), and 20 ng total RNA was used for each library. RNA samples were processed with an Illumina TruSeq RNA

Access Library prep kit, following the manufacturers instructions. Libraries were quantified with Qubit HS (ThermoFisher) and Fragment Analyzer (Advanced Analytical Technologies). Indexed libraries were pooled and sequenced on an Illumina NextSeq 500 using paired-end chemistry with 75 bp read length.

For analysis, the raw RNA sequences were quality assessed using FASTQC and no further trimming was performed. The latest mouse transcript set (release 87, "REL87") was obtained by ftp from ensembl (ftp://ftp.ensembl.org/pub/release-87/fasta/mus_musculus/), and annotation acquired using BioMart. Transcripts for both cDNA and ncRNA were used. Alignments (--end-to-end, --very-sensitive -p 30 --no-unal --no-discordant settings) to the REL87 reference set were performed using bowtie2 (version 2.2.7). Alignments were stored in indexed BAM files. Normalized data provided the input for statistical hypothesis testing, in which we sought to identify loci that were statistically significantly different between sample groups. We were also interested in the degree of difference, i.e. the fold-change. In the outputs, the fold-changes (logFC) are given as log2 values, with a positive logFC representing up-regulation, and a negative logFC indicating down-regulation. For each comparison, the first group (A) is the numerator, while the second group (B) is the denominator. Thus, a positive logFC for the comparison 'A-B' indicates up-regulation in A relative to B. Comparisons, manually chosen to explore the data, were undertaken using linear modelling. Subsequently, empirical Bayesian analysis was applied (including vertical (within a given comparison) *P* value adjustment for multiple testing, which controls for false discovery rate). For each comparison, the null hypothesis was that there was no difference between the groups being compared. The Bioconductor package limma was used and an overview of the underlying biological changes occurring within each comparison obtained by functional enrichment analysis from KEGG pathway membership. The significance threshold for functional analysis was manually chosen to be $p<0.01$

Quantitative PCR

Post-culture macrophages were lysed in the plate using RLT lysis buffer and RNA was isolated with RNeasy microkits (Qiagen) according to the manufacturers instructions. cDNA was generated from extracted RNA using SuperScript-III and Oligo-dT (ThermoFisher). Relative quantification of genes of interest was performed by qPCR analysis using QuantStudio 12K Flex system and SYBR Green master mix (ThermoFisher), compared with a serially diluted standard of pooled cDNA. Expression was normalized to β-actin (primers as in Table S8).

Seahorse extracellular flux analysis

FACS isolated PECMs or AlvMs from a pool of 8 mice were plated at 150,000 cells per well and allowed to adhere for at least 1h. ECAR and OCR were measured in XF media (modified DMEM containing 2 mM l-glutamine) under basal conditions, in response to 25 mM glucose, 20 μM oligomycin, 100 mM 2-DG (ECAR) or 20μM Oligomycin, 15μM FCCP, 10μM Antimycin A, 1μM Rotenone (OCR) (Sigma) using a 96-well extracellular flux analyzer XFe-96 (Seahorse Bioscience).

Statistical analysis

Data are shown as mean values ± S.E.M. Where applicable, data were analyzed by unpaired *t* test, one-way or two-way ANOVA with Tukey's post-test as appropriate. Significant differences were defined at $P<0.05$. Statistical analysis was performed using GraphPad PRISM version 7.

Reporting Summary

Further information on research design and reagents is available in the Life Sciences Reporting Summary linked to this article.

Code availability statement

Bioinformatics analyses was performed with publicly available code from bioconductor.org.

Data Availability

The data that support the findings of this study are available from the corresponding author upon request. RNA-seq data were deposited at Gene Expression Omnibus, with the following accession code: GSE126309.

Method References

51. Finkelman, F.D. *et al.* Anti-cytokine antibodies as carrier proteins. Prolongation of in vivo effects of exogenous cytokines by injection of cytokine-anti-cytokine antibody complexes. *Journal of immunology* **151**, 1235-1244 (1993).
52. Cook, P.C. *et al.* A dominant role for the methyl-CpG-binding protein Mbd2 in controlling Th2 induction by dendritic cells. *Nature communications* **6**, 6920 (2015).
53. Anderson, K.G. *et al.* Intravascular staining for discrimination of vascular and tissue leukocytes. *Nat Protoc* **9**, 209-222 (2014).
54. Bain, C.C. *et al.* Resident and pro-inflammatory macrophages in the colon represent alternative context-dependent fates of the same Ly6Chi monocyte precursors. *Mucosal Immunol* **6**, 498-510 (2013).
55. Phythian-Adams, A.T. *et al.* CD11c depletion severely disrupts Th2 induction and development in vivo. *The Journal of experimental medicine* **207**, 2089-2096 (2010).
56. Wilhelm, C. *et al.* Critical role of fatty acid metabolism in ILC2-mediated barrier protection during malnutrition and helminth infection. *The Journal of experimental medicine* **213**, 1409-1418 (2016).
57. Evans, C.M. *et al.* The polymeric mucin Muc5ac is required for allergic airway hyperreactivity. *Nature communications* **6**, 6281 (2015).
58. Schneider, C.A., Rasband, W.S. & Eliceiri, K.W. NIH Image to ImageJ: 25 years of image analysis. *Nature methods* **9**, 671-675 (2012).

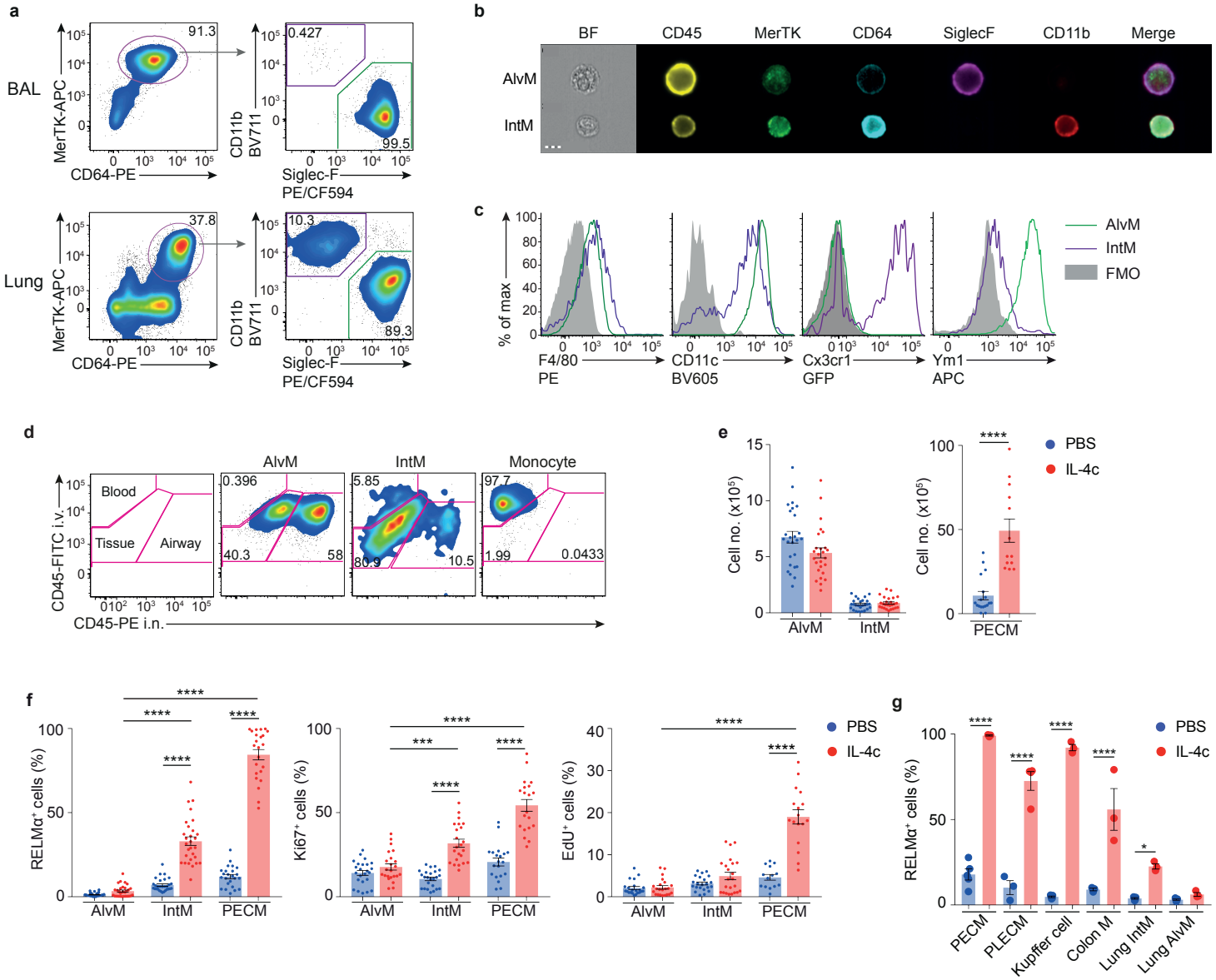
a
BAL
Lung
MerTK-APC
CD64-PE
CD11b BV711
Siglec-F PE/CF594
91.3
0.427
99.5
37.8
10.3
89.3
b
BF
CD45
MerTK
CD64
SiglecF
CD11b
Merge
AlvM
IntM
c
% of max
F4/80 PE
CD11c BV605
Cx3cr1 GFP
Ym1 APC
AlvM
IntM
FMO
d
Blood
Tissue
Airway
CD45-FITC i.v.
CD45-PE i.n.
AlvM
IntM
Monocyte
0.396
40.3
58
5.85
80.9
10.5
97.7
1.99
0.0433
e
Cell no. (x10⁵)
AlvM
IntM
PECM
PBS
IL-4c
f
RELMα⁺ cells (%)
Ki67⁺ cells (%)
EdU⁺ cells (%)
AlvM
IntM
PECM
PBS
IL-4c
g
RELMα⁺ cells (%)
PECM
PLECM
Kupffer cell
Colon M
Lung IntM
Lung AlvM
PBS
IL-4c

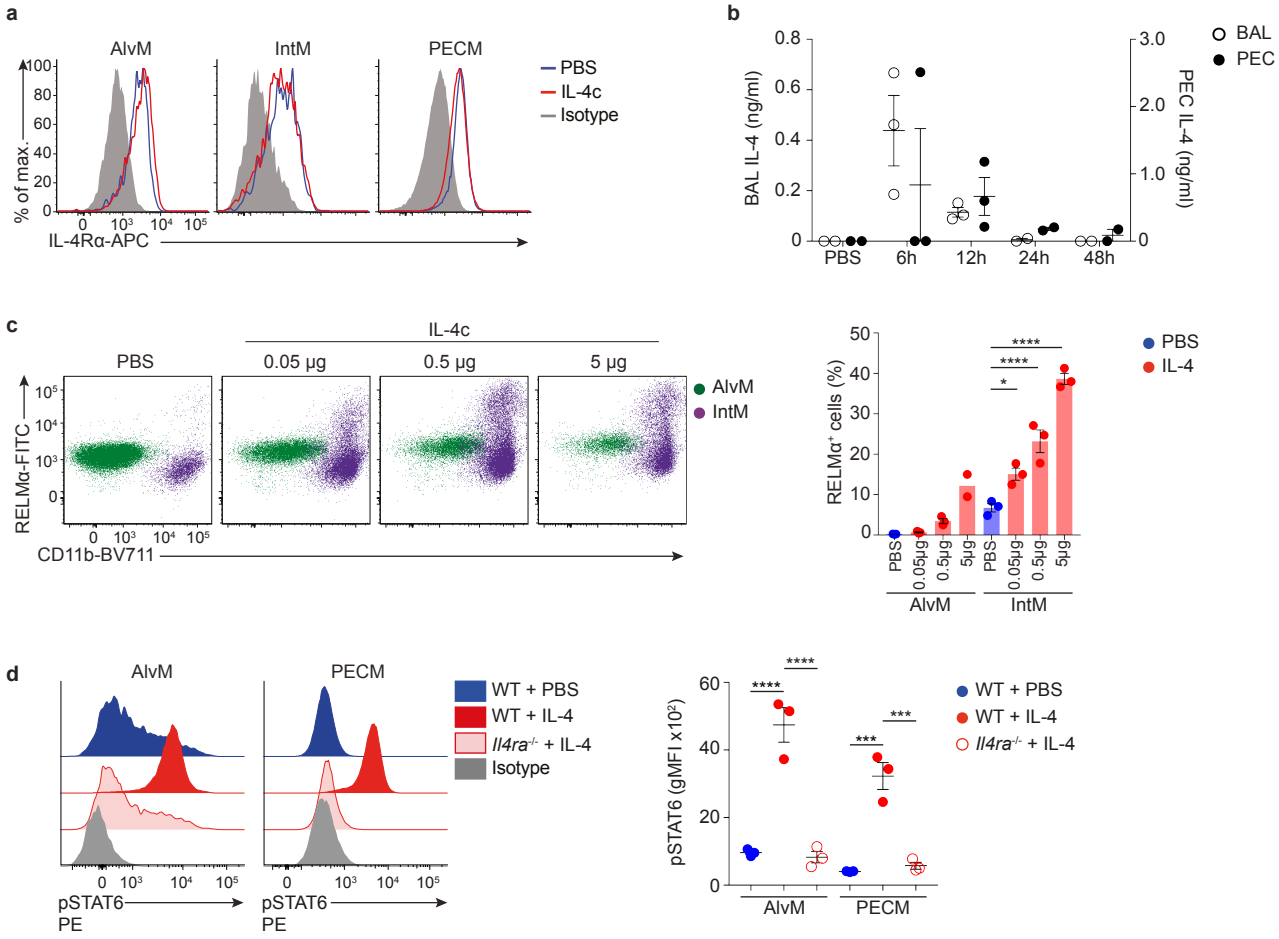
a
AlvM
IntM
PECM
PBS
IL-4c
Isotype
% of max.
IL-4Rα-APC
b
BAL
PEC
BAL IL-4 (ng/ml)
PEC IL-4 (ng/ml)
PBS
6h
12h
24h
48h
c
IL-4c
PBS
0.05 µg
0.5 µg
5 µg
AlvM
IntM
RELMα-FITC
CD11b-BV711
RELMα⁺ cells (%)
PBS
IL-4
AlvM
IntM
d
AlvM
PECM
WT + PBS
WT + IL-4
Il4ra-/- + IL-4
Isotype
pSTAT6 PE
pSTAT6 (gMFI x10²)
AlvM
PECM

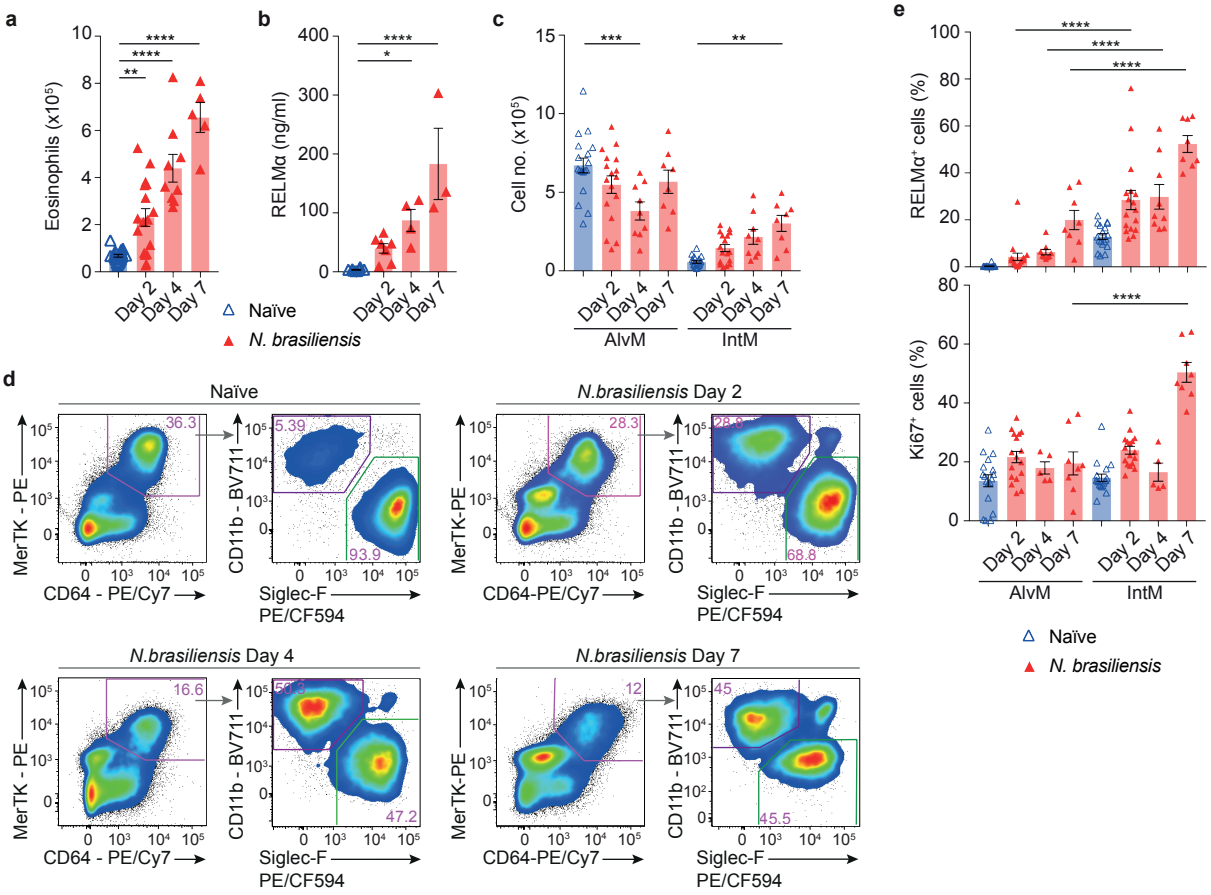
a
Eosinophils (x10⁵)
b
RELMα (ng/ml)
c
Cell no. (x10⁵)
AlvM
IntM
Day 2
Day 4
Day 7
Naïve
N. brasiliensis
d
Naïve
N.brasiliensis Day 2
N.brasiliensis Day 4
N.brasiliensis Day 7
MerTK - PE
CD64 - PE/Cy7
CD11b - BV711
Siglec-F PE/CF594
36.3
5.39
93.9
28.3
68.8
16.6
47.2
12
45
45.5
e
RELMα⁺ cells (%)
Ki67⁺ cells (%)

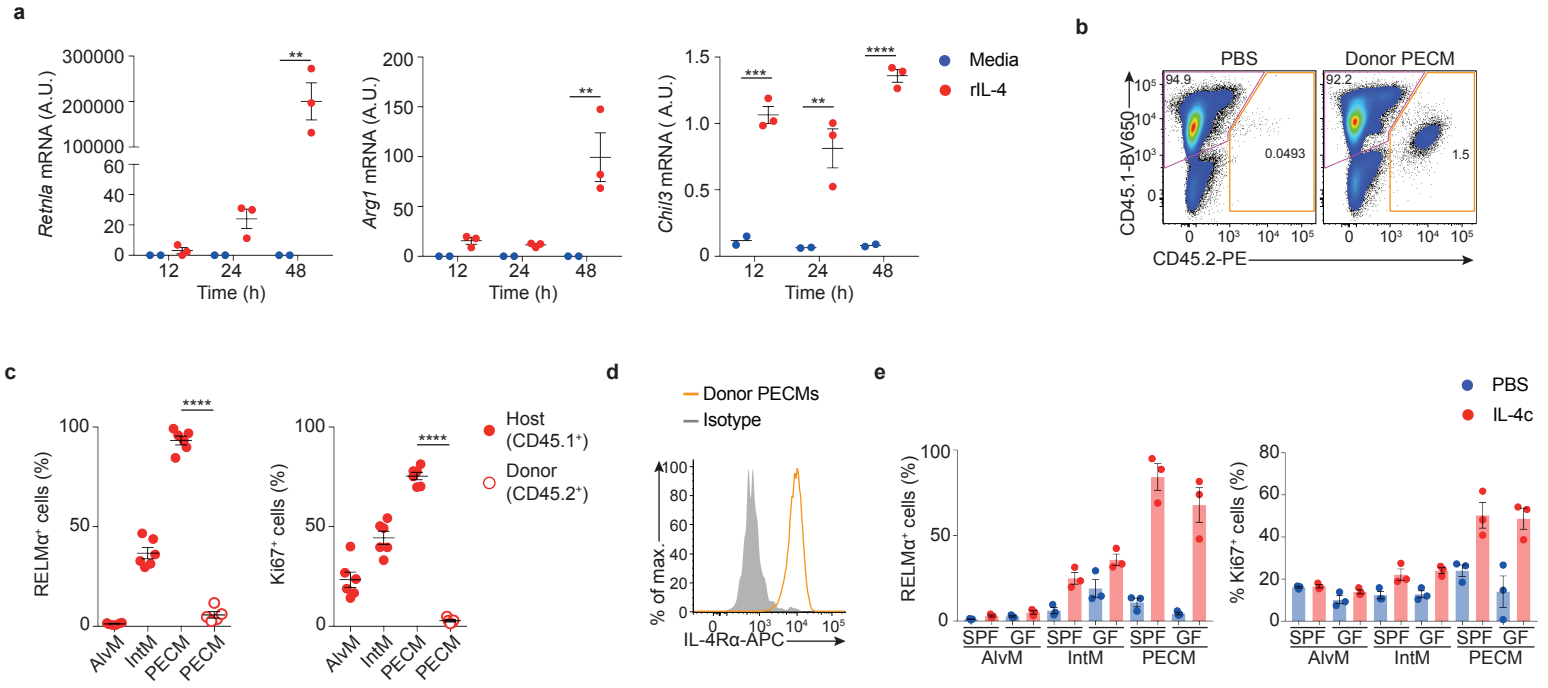
a
Retnla mRNA (A.U.)
Arg1 mRNA (A.U.)
Chil3 mRNA (A.U.)
Time (h)
Media
rIL-4
b
PBS
Donor PECM
CD45.1-BV650
CD45.2-PE
94.9
0.0493
92.2
1.5
c
RELMα⁺ cells (%)
Ki67⁺ cells (%)
AlvM
IntM
PECM
Host (CD45.1⁺)
Donor (CD45.2⁺)
d
Donor PECMs
Isotype
% of max.
IL-4Rα-APC
e
PBS
IL-4c
RELMα⁺ cells (%)
% Ki67⁺ cells (%)
SPF
GF

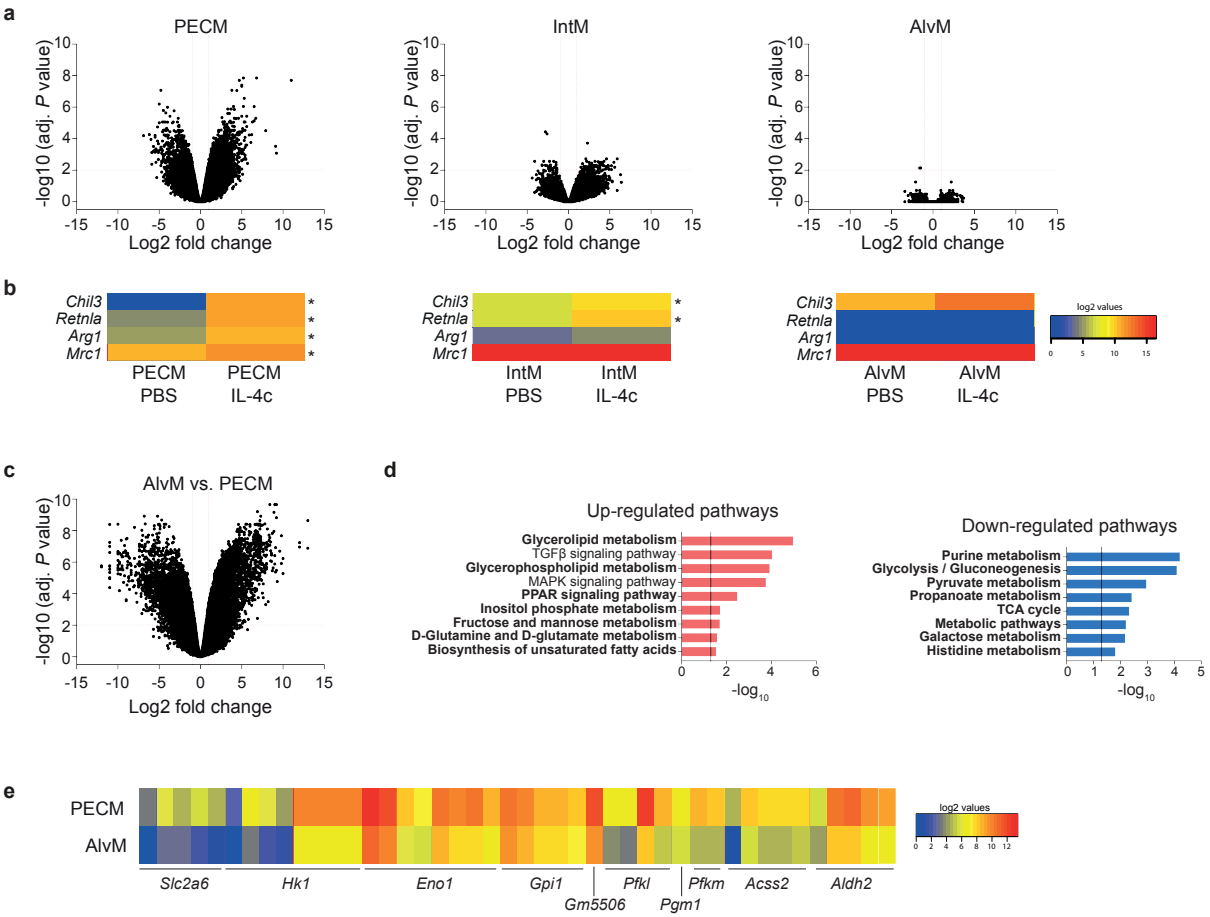
a
PECM
IntM
AlvM
-log10 (adj. P value)
Log2 fold change
b
Chil3
Retnla
Arg1
Mrc1
PECM PBS
PECM IL-4c
IntM PBS
IntM IL-4c
AlvM PBS
AlvM IL-4c
log2 values
c
AlvM vs. PECM
d
Up-regulated pathways
Glycerolipid metabolism
TGFβ signaling pathway
Glycerophospholipid metabolism
MAPK signaling pathway
PPAR signaling pathway
Inositol phosphate metabolism
Fructose and mannose metabolism
D-Glutamine and D-glutamate metabolism
Biosynthesis of unsaturated fatty acids
Down-regulated pathways
Purine metabolism
Glycolysis / Gluconeogenesis
Pyruvate metabolism
Propanoate metabolism
TCA cycle
Metabolic pathways
Galactose metabolism
Histidine metabolism
e
PECM
AlvM
Slc2a6
Hk1
Eno1
Gpi1
Pfkl
Pfkm
Acss2
Aldh2
Gm5506
Pgm1

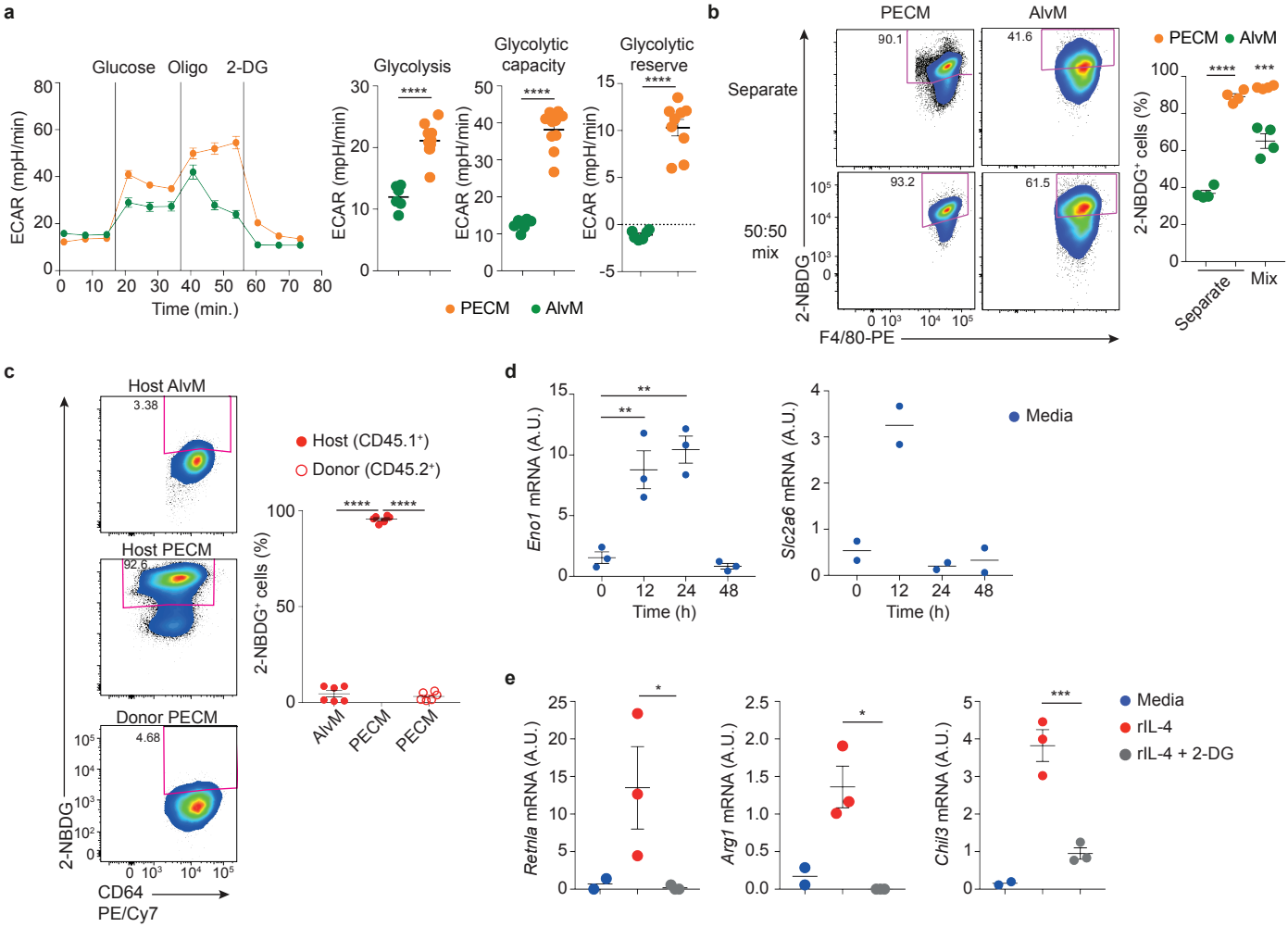
a
Glucose
Oligo
2-DG
ECAR (mpH/min)
Time (min.)
Glycolysis
Glycolytic capacity
Glycolytic reserve
PECM
AlvM
b
PECM
AlvM
Separate
50:50 mix
90.1
41.6
93.2
61.5
2-NBDG
F4/80-PE
2-NBDG⁺ cells (%)
Separate
Mix
c
Host AlvM
Host PECM
Donor PECM
3.38
92.6
4.68
2-NBDG
CD64
PE/Cy7
Host (CD45.1⁺)
Donor (CD45.2⁺)
2-NBDG⁺ cells (%)
AlvM
PECM
PECM
d
Eno1 mRNA (A.U.)
Slc2a6 mRNA (A.U.)
Time (h)
Media
e
Retnla mRNA (A.U.)
Arg1 mRNA (A.U.)
Chil3 mRNA (A.U.)
Media
rIL-4
rIL-4 + 2-DG